

## Impurity Effect on Surface Diffusion: CO/S/Ni(110)

Xu-Dong Xiao, Yuanlin Xie, Christian Jakobsen, Heather Galloway, Miquel Salmeron, and Y. R. Shen

*Department of Physics, University of California  
and Materials Science Division, Lawrence Berkeley Laboratory, Berkeley, California 94720*

(Received 31 October 1994)

Macroscopic CO diffusion on Ni(110) was found to be greatly impeded by surface contamination of just a few percent of a sulfur monolayer. The effect became even much more pronounced if the sample was annealed at high temperatures. The results can be understood from the consideration that S-covered steps can effectively block CO diffusion with a much higher energy barrier.

PACS numbers: 68.45.-v, 68.35.Fx

Surface diffusion can be affected by impurities [1–5]. Earlier studies indicate that impurities could both enhance and impede surface self-diffusion [1,2]. In the few cases where the effects of low coverages [ $\sim 0.1$  monolayer (ML)] were examined, no significant changes in the self-diffusivities were observed [2]. One might expect that the same could be true for heterogeneous (macroscopic or chemical) surface diffusion. However, measurements have indicated a fairly strong impurity effect in the latter case, although the experimental data are limited, usually at one or two temperatures only [4,5]. Two models have been proposed to explain the limited experimental observations. One suggests that impurities may modify specific surface sites (e.g., step sites) and therefore affect the measured overall diffusion coefficient [4]. Indeed, it was reported in a recent paper dealing with surfactant effect on epitaxial growth that oxygen could reduce the Schwoebel energy barrier for Pt self-diffusion on Pt(111) at step sites [4(b)]. The other assumes the existence of some “long-range” impurity effect on the surface potential [5]. Quantitative comparison between theory and experiment is, however, difficult because of the lack of complete sets of measurement. Consequently, no clear understanding of the impurity effect on surface diffusion has yet been obtained.

Recently, we have developed the method of optical diffraction from monolayer gratings to study surface diffusion. It has a number of advantages over conventional techniques [6]. In particular, its sensitivity allows us to probe impurity effects on anisotropic surface diffusion with different coverages. We have used the technique to study CO diffusion on S contaminated Ni(110) surfaces. It is well known that S is poisonous to the catalytic methanation reaction on transition metals [7]. A study of diffusion characteristics of the system may shed some light on the catalytic deactivation mechanism. We have found that even a small amount of S impurity can strongly impede CO diffusion on Ni(110). The apparent activation energy  $E_D$  for CO diffusion along  $[1\bar{1}0]$  increases monotonically from 2.2 kcal/mol for a clean surface to 6.2 kcal/mol at 0.05 ML S coverage and reaches the saturation value of 7.5 kcal/mol at  $\sim 0.1$  ML S coverage. If the surface is annealed at high temperatures ( $\sim 1120$  K) after S deposition,

then  $E_D$  increases to 6.0 kcal/mol with only 0.01 ML of S and saturates at about 0.02 ML of S. For CO diffusion along  $[001]$ ,  $E_D$  also increases from 2.8 kcal/mol for a clean surface to 7.0 kcal/mol at 0.05 ML S coverage and reaches the saturation value of 7.5 kcal/mol at 0.1 ML S coverage, but exhibits little effect from annealing. The results can be understood by a S-modified step-controlled diffusion model, including the possibility of S-induced step morphology change by annealing. Scanning tunneling microscopy (STM) measurement supports this conjecture.

The experiment was performed in an ultrahigh vacuum (UHV) chamber with a base pressure of  $2.0 \times 10^{-10}$  torr. A single crystal of Ni(110), cut and mechanically polished to within  $0.2^\circ$  of the (110) plane, was used for the measurement. Its surface was cleaned by  $\text{Ar}^+$  sputtering at room temperature, followed by annealing at 1120 K for 10 min, a slow cooling of  $\sim 0.5$  K/sec to 800 K, and then a more rapid cooling of  $\sim 2$  K/sec to room temperature. Auger spectra of the clean surface showed no detectable impurities ( $<0.5\%$  S and C, and  $<1\%$  O). Observation of a sharp  $(1 \times 1)$  low energy electron diffraction (LEED) pattern from a clean Ni(110) surface and  $(2 \times 1)$  from a full CO monolayer on Ni(110) ensured that the surface was well ordered. The sample temperature was monitored by a thermocouple and controlled to within  $\pm 1$  K.

The surface S impurities were introduced in two different ways: one by heating the nickel sample at 1120 K for an extended period of time, typically 1 h, to obtain 0.01 ML of S from bulk segregation, and the other by dosing  $\text{H}_2\text{S}$  onto Ni(110) at room temperature with a subsequent brief annealing at 650 K to desorb hydrogen resulting from  $\text{H}_2\text{S}$  dissociation. The concentration of S was measured by the intensity change of the 152 eV S peak in the Auger spectrum normalized to that of the saturation coverage of  $\theta_S = 0.67$  ML corresponding to a  $p(3 \times 2)$  structure at room temperature [8]. The S atoms were known to desorb only at very high temperatures (above 1200 K) [9]. A brief flashing of the sample to 650 K was sufficient to desorb CO but did not affect the S coverage. In the experiment, we first covered the Ni(110) surface with the desired amount of S, and then

dosed it with CO at 160 K to a saturation coverage, thus maintaining a constant local CO configuration for various S coverages [10].

The optical technique for surface diffusion measurements has been described elsewhere [6]. In short, two 1.06  $\mu\text{m}$  pulsed laser beams were made to interfere on the CO-covered Ni surface to create by laser thermal desorption a CO monolayer grating with a modulation depth of  $\Delta\theta_{\text{CO}} \sim 0.03$  ML and a grating spacing of  $\sim 3 \mu\text{m}$ . Then a polarization-modulation scheme was used to monitor linear optical diffraction from the grating. The decay of the first-order diffraction signal directly reflects how the grating is smeared by diffusion and is related to the surface diffusion coefficient  $D$  by

$$S(t) = S_0 \exp(-8\pi^2 D t / s^2), \quad (1)$$

where  $s$  is the grating spacing and  $S_0$  is the initial signal strength.

The measured CO diffusion coefficient as a function of inverse temperature  $1/T$  is plotted in Figs. 1(a) and 1(b) for diffusion along  $[1\bar{1}0]$  and  $[001]$ , respectively, for several S coverages prepared by  $\text{H}_2\text{S}$  dosing. That CO dif-

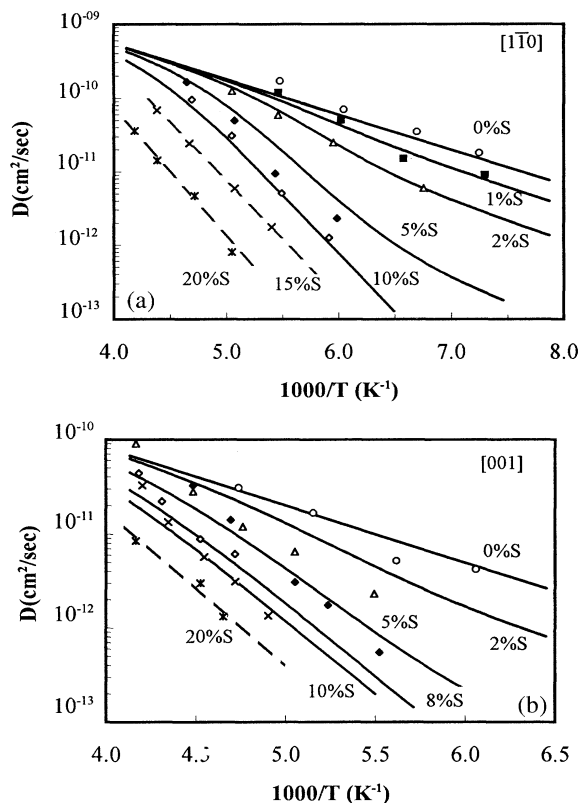


FIG. 1. (a) CO diffusion coefficient along  $[1\bar{1}0]$  as a function of the reciprocal temperature for a number of S coverages: 0% S, 1% S, 2% S, 5% S, 10% S, 15% S, and 20% S. The solid lines are theoretical curves. The dashed lines at high S coverages are a guide for the eye. (b) Similar to (a) for CO diffusion along  $[001]$  for a number of S coverages: 0% S, 2% S, 5% S, 8% S, 10% S, and 20% S.

fusion is strongly impeded by sulfur impurities is already obvious at S coverage of  $\theta_S = 0.01$  ML. Fitting the data to the Arrhenius form  $D = D_0 \exp(-E_D/kT)$  yields the apparent diffusion activation energy  $E_D$  and the preexponential factor  $D_0$ . We show in Figs. 2(a) and 2(b), respectively,  $E_D$  and  $D_0$  versus  $\theta_S$  for CO diffusion in the  $[1\bar{1}0]$  direction. Note that  $E_D$  increases monotonically from the clean surface value of 2.2 kcal/mol to a saturation value of 7.5 kcal/mol at  $\theta_S \sim 0.1$  ML. Further decrease of  $D$  for higher  $\theta_S$  comes from a decrease of  $D_0$ .

The impurity effect on CO diffusion along  $[1\bar{1}0]$  was found to be much stronger if the S impurity coverages were prepared by bulk segregation through heating. As shown in Fig. 2,  $E_D$  now increases to 6.2 kcal/mol at  $\theta_S \sim 0.01$  ML as compared to 2.8 kcal/mol in the previous case and saturates at  $\theta_S \sim 0.02$  ML. The difference between the two cases seems to result from high-temperature annealing of the sample. Indeed, the same stronger impurity effect was observed when the S-covered Ni(110) surfaces prepared by  $\text{H}_2\text{S}$  deposition were heated to 1120 K for 2 to 12 min. This is also shown in Fig. 2. For CO diffusion along  $[001]$ , however, no significant differences were

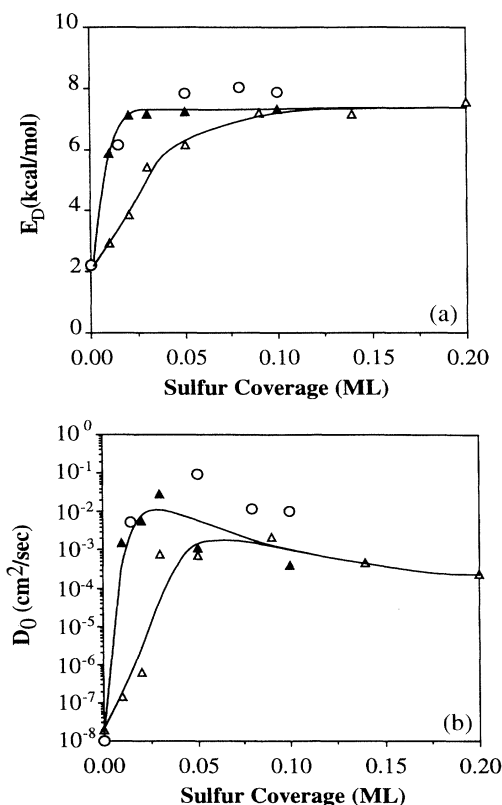


FIG. 2. CO diffusion activation energy (a) and preexponential factor (b) as a function of S impurity coverage. The open and filled triangles are for samples without and with high-temperature annealing, respectively, after dosing with  $\text{H}_2\text{S}$ . The open circles are for samples with surface S obtained by bulk segregation. The solid lines are a guide for the eye.

observed between S impurities prepared by bulk segregation and by H<sub>2</sub>S deposition with or without further annealing. Thus high-temperature annealing, which does not affect impurity coverages as monitored by Auger electron spectroscopy (AES), must have altered the surface structure to modify mostly CO diffusion along [1 $\bar{1}$ 0].

It is known from thermal desorption spectroscopy that a weak repulsive interaction exists between CO and S. This S-CO interaction cannot be responsible for our observations since it would lead to a decrease rather than an increase of  $E_D$  as  $\theta_S$  increases. A long-range interaction model also does not work because it would require a significant change in the potential of  $\sim 30$  CO adsorption sites by each S atom to explain the observed results, while all theoretical calculations predict that the effect of S on the substrate surface cannot extend beyond the next-nearest neighbors [11]. [We note that S atoms on Ni(110) are not highly mobile at our measurement temperatures [9].] An alternate plausible model assumes that the S impurities occupy the step sites and modify the step potentials, leading to step-controlled surface diffusion.

We have performed STM measurements on our Ni(110) sample which had a miscut of  $\sim 0.2^\circ$  along the direction about  $25^\circ$  from [1 $\bar{1}$ 0] (see Fig. 3). We have confirmed the previous findings of S diffusing readily on Ni(110) at room temperature and preferentially occupying the step sites [12]. The STM images showed a step density of  $\sim 20$  steps/ $\mu\text{m}$ ,  $\sim \frac{2}{3}$  of which were along the miscut direction,  $\sim \frac{1}{6}$  along [1 $\bar{1}$ 0],  $\sim \frac{1}{30}$  along [001], and  $\sim \frac{1}{7}$  along the diagonals of the surface unit cells. This gives an average spacing between two neighboring steps of  $\sim 1300$  Å along [1 $\bar{1}$ 0] and  $\sim 600$  Å along [001]. Assuming all step sites are covered by S at a S coverage of 0.1 ML, a simple calculation shows that the adsorption energy of S on the step sites

is  $\sim 3$  kcal/mol larger than that on the terrace sites, which seems reasonable [13]. For step-influenced diffusion with all step sites covered by S, the diffusion coefficient  $D$  measured by our technique is expected to take the form [14]

$$D = [(L_0 - a)^2/L_0^2 D_t + a^2/L_0^2 D_s]^{-1}, \quad (2)$$

where  $D_t$  and  $D_s$  are diffusion constants for diffusion on the terraces and across the S-covered steps, respectively,  $a$  is the lattice constant, and  $L_0$  is the average spacing between two neighboring steps in the diffusion direction. With  $D_t = D_{t0} \exp(-E_t/kT)$  and  $D_s = D_{s0} \exp(-E_s/kT)$ , the step-controlled diffusion, denoted by  $D \dot{\sim} (L_0^2/a^2)D_s$ , should occur when  $\exp[(E_s - E_t)/kT] \gg (D_{s0}/D_{t0})(L_0/a)^2$ . We find that the experimental data for 0.1 ML of S in Fig. 1 can indeed be well described by step-controlled diffusion with  $D_{s0}(1\bar{1}0) = 1.8 \times 10^{-8}$  cm<sup>2</sup>/sec,  $D_{s0}(001) = 6.0 \times 10^{-9}$  cm<sup>2</sup>/sec, and  $E_s(001) = E_s(1\bar{1}0) = 7.5$  kcal/mol, knowing that  $L_0 = 1300$  Å and  $a = 2.5$  Å along [1 $\bar{1}$ 0] and  $L_0 = 600$  Å and  $a = 3.5$  Å along [001]. From the data for 0% S in Fig. 1, we obtain  $D_{t0}(1\bar{1}0) = 4.4 \times 10^{-8}$  cm<sup>2</sup>/sec,  $D_{t0}(001) = 2.2 \times 10^{-8}$  cm<sup>2</sup>/sec,  $E_t(1\bar{1}0) = 2.2$  kcal/mol, and  $E_t(001) = 2.8$  kcal/mol. It is then reassuring to see that the condition for step-controlled CO diffusion with 0.1 ML of S is indeed satisfied in the temperature range of our measurement. We note that the effect of steps on CO diffusion on our clean Ni(110) sample was negligible following Eq. (2) because from a separate measurement on clean stepped Ni(110) surfaces we found  $E_s \sim 5.5$  kcal/mol in the absence of S.

The observation of a stronger S impurity effect on CO diffusion along [1 $\bar{1}$ 0] after high-temperature (1120 K) annealing can be understood by the observed step morphology change induced by heating with the presence of more than 0.01 ML of S. Our STM images [see Fig. 3(b)] showed no surface structural changes except that the steps

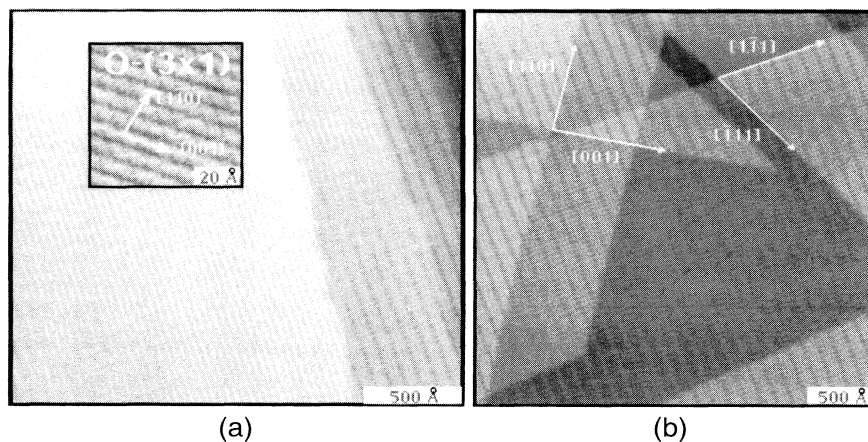


FIG. 3. (a) STM image ( $2350 \times 2180$  Å<sup>2</sup>) of a clean Ni(110) surface with a  $0.2^\circ$  miscut, showing steps along the miscut direction. The inset shows the Ni(110)-O( $3 \times 1$ ) structure when the surface was covered by oxygen. The oxygen rows along [001] help determine the crystallographic directions. (b) STM image ( $3140 \times 3340$  Å<sup>2</sup>) of Ni(110) exposed to 20 L of H<sub>2</sub>S and then annealed at high temperature (1100 K). Steps now appear along the diagonals [1 $\bar{1}$ 1] and [1 $\bar{1}$ 1] of the surface unit cell as well as along [001] and [1 $\bar{1}$ 0].

perpendicular to the surface miscut direction had been replaced by  $\sim 5$  steps/ $\mu\text{m}$  along each diagonal direction of the surface unit cell and additional ones (10 steps/ $\mu\text{m}$ ) along  $[1\bar{1}0]$ . The observed saturation of  $E_D$  along  $[1\bar{1}0]$  at a lower S coverage  $\theta_S \sim 0.02$  ML as compared to  $\theta_S \sim 0.1$  ML before annealing suggests that S must have adsorbed at these diagonal steps more readily to have such sites all covered by S at  $\theta_S \sim 0.02$  ML. With the effective terrace width along  $[1\bar{1}0]$  basically unchanged, CO diffusion along  $[1\bar{1}0]$  could now be controlled by the S-covered steps at  $\theta_S \sim 0.02$  ML. However, these S-covered diagonal steps resulted in  $L_0 \sim 1800$  Å along  $[001]$ , so that the condition for step-controlled CO diffusion along  $[001]$  was not yet satisfied. To have the condition satisfied, the steps along  $[1\bar{1}0]$  must also be covered by S as in the situation before annealing that could occur only at  $\theta_S \sim 0.1$  ML. This is presumably the reason behind the hardly noticeable effect of annealing on CO diffusion along  $[001]$  on S-covered Ni(110).

We can construct a model to quantitatively explain our results. Let  $\gamma\theta_S$  be the fraction of step sites covered by S at coverage  $\theta_S$ . The average spacing between two neighboring S-covered steps is then given by  $L(\theta_S) = L_0/\gamma\theta_S$ . We expect that Eq. (2) still holds with  $L_0$  replaced by  $L(\theta_S)$ . However,  $D_s$  should now consist of two parts:  $D_s = D_I + D_{II}$  with  $D_I = D_{s0} \exp(-E_s/kT)$  describing diffusion directly across the S-covered steps, and  $D_{II}$  describing diffusion via a detour around the S-covered part of the steps (see Fig. 4). Since  $D_{II}$  must vanish when all the step sites are covered by S, we assume  $D_{II} = (1 - \gamma\theta_S)^n D'_{II}$ , and find that  $n = 2$  can fit the data fairly well, but not  $n = 1$ . We then also have a more symmetric form for the  $D_s$  term in Eq. (2),

$$\frac{L(\theta_S)^2}{a^2} D_s = \frac{L_0^2}{a^2} \left( \frac{1}{(\gamma\theta_S)^2} D_I + \frac{(1 - \gamma\theta_S)^2}{(\gamma\theta_S)^2} D'_{II} \right). \quad (3)$$

Since the  $D_{II}$  part basically describes a distortion of the diffusion pathways on the terraces, we simply assume  $D'_{II} = D'_{II0} \exp(-E_t/kT)$  with  $E_t = 2.5$  kcal/mol being an average of  $E_t(1\bar{1}0)$  and  $E_t(001)$ . We can then use Eqs. (2) and (3) with  $D'_{II0}$  as the only adjustable parameter in fitting the data in Fig. 1, as  $D_t$  and  $D_I$  have already been determined from the results with  $\theta_S = 0$  and  $\theta_S = 0.1$  ML, respectively. We find that with  $D'_{II0} = 7.0 \times 10^{-15}$  cm<sup>2</sup>/sec. The agreement between theory and experiment appears satisfactory, as shown in Fig. 1. For  $\theta_S > 0.1$  ML, the effect of S on CO diffusion on terraces may become significant. It is likely that S impurities on terraces simply act as road blocks to CO diffusion and thus lengthen the CO diffusion pathways. Then the effect only appears as a reduction of the preexponential factor  $D_0$ , as shown by Mak and co-workers [5].

In summary, we have studied experimentally the S impurity effects on anisotropic CO diffusion on Ni(110). We have found that a few percent of a monolayer of S can drastically reduce the CO diffusion rate. S-covered steps appear to be responsible for impeding the CO diffusion.

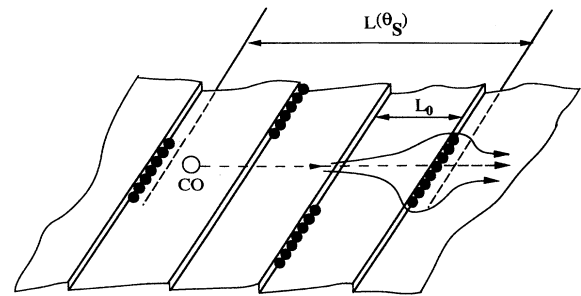


FIG. 4. Schematic showing particle diffusion on a stepped surface with the steps partially covered by impurities.

A simple heuristic model can be used to explain the observations quantitatively. Our findings here suggest that for intrinsic surface diffusion studies to be reliable, it is important to keep the surface clean to a very high level.

This work was supported by the Director, Office of Energy Research, Office of Basic Energy Sciences, Materials Sciences Division of the U.S. Department of Energy under Contract No. DE-ACO3-76SF00098.

- [1] J. Perdereau and G.E. Rhead, *Surf. Sci.* **7**, 175 (1967); F. Delamare and G.E. Rhead, *ibid.* **28**, 267 (1971); H. Roux, A. Piquet, R. Uzan, and M. Drechsler, *ibid.* **59**, 97 (1976); H. Roux, A. Piquet, G. Pralong, R. Uzan, and M. Drechsler, *ibid.* **71**, 375 (1978).
- [2] M. Pichaud and M. Drechsler, *Surf. Sci.* **32**, 341 (1972); **36**, 813 (1973).
- [3] L.D. Schmidt and R. Gomer, *J. Chem. Phys.* **43**, 95 (1965); A.J. Melmed, *J. Appl. Phys.* **37**, 275 (1966); R. Blaszczyszyn and Ch. Kleint, *Surf. Sci.* **253**, 129 (1991).
- [4] (a) R. Morin and M. Drechsler, *Surf. Sci.* **111**, 140 (1981). (b) S. Esch, M. Hohage, T. Michely, and G. Comsa, *Phys. Rev. Lett.* **72**, 518 (1994).
- [5] J.L. Brand, A.A. Deckert, and S.M. George, *Surf. Sci.* **194**, 457 (1988); C.H. Mak, B.G. Koehler, J.L. Brand, and S.M. George, *J. Chem. Phys.* **87**, 2340 (1987).
- [6] X.-D. Xiao, Y. Xie, and Y.R. Shen, *Surf. Sci.* **271**, 295 (1992).
- [7] M.P. Kiskinova, *Surf. Sci. Rep.* **8**, 359 (1988); R.J. Madix, *Catal. Rev. Sci. Eng.* **26**, 281 (1984); J. Oudar, *ibid.* **22**, 171 (1980).
- [8] F. Besenbacher, I. Stensgaard, L. Rusan, J.K. Norskov, and K.W. Jacobsen, *Surf. Sci.* **272**, 334 (1992); D.R. Huntley, *ibid.* **240**, 13 (1990).
- [9] M. Blaszczyszyn, R. Blaszczyszyn, R. Meclowski, A.J. Melmed, and T.E. Madey, *Surf. Sci.* **131**, 433 (1983).
- [10] X.-D. Xiao, Y. Xie, and Y.R. Shen, *Phys. Rev. B* **48**, 17452 (1993).
- [11] P.J. Feibelman, *Annu. Rev. Phys. Chem.* **40**, 261 (1989), and references therein.
- [12] P. Sprunger, F. Besenbacher, I. Stensgaard, and E. Laegsgaard (private communication).
- [13] G. Samojai, *Chemistry in Two Dimensions: Surfaces* (Cornell University Press, Ithaca, 1981).
- [14] X.-D. Xiao, X.D. Zhu, W. Daum, and Y.R. Shen, *Phys. Rev. B* **46**, 9732 (1992).

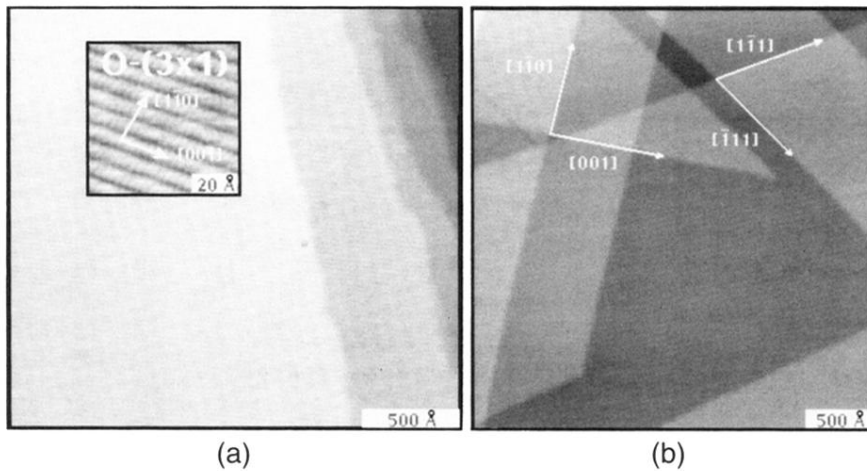


FIG. 3. (a) STM image ( $2350 \times 2180 \text{ \AA}^2$ ) of a clean Ni(110) surface with a  $0.2^\circ$  miscut, showing steps along the miscut direction. The inset shows the Ni(110)-O( $3 \times 1$ ) structure when the surface was covered by oxygen. The oxygen rows along [001] help determine the crystallographic directions. (b) STM image ( $3140 \times 3340 \text{ \AA}^2$ ) of Ni(110) exposed to 20 L of H<sub>2</sub>S and then annealed at high temperature (1100 K). Steps now appear along the diagonals  $[\bar{1}11]$  and  $[1\bar{1}1]$  of the surface unit cell as well as along [001] and  $[\bar{1}10]$ .